

Adsorption Mechanism of Heavy Metals Using Activated Carbon Derived from *Hydrilla Verticillata*

Enda Rasilta Tarigan^{1,2}, Erna Frida^{1,*}, Syahrul Humaidi¹ and Susilawati¹

¹Post Graduate Program (Physics), FMIPA, Universitas Sumatera Utara, Sumatera Utara 20155, Indonesia

²Politeknik Teknologi Kimia Industri, Sumatera Utara 20228, Indonesia

(*Corresponding author's e-mail: ernafridatarigan@usu.ac.id)

Received: 22 July 2024, Revised: 6 August 2024, Accepted: 13 August 2024, Published: 1 November 2024

Abstract

This research investigates the adsorption mechanism of heavy metals (Cu, Pb, Fe and Zn) using activated carbon derived from *Hydrilla verticillata*, addressing the critical issue of water pollution caused by heavy metals, which pose significant environmental and health risks due to their persistence and toxicity. The study outlines the preparation process of the activated carbon, which involves washing, drying, carbonization, chemical activation and hydrothermal treatment. Characterization through SEM, EDX, XRD and FTIR analyses confirms the presence of functional groups and an amorphous structure conducive to adsorption. Adsorption tests reveal that *H. verticillata*-derived activated carbon shows high removal efficiency, especially for lead (Pb), with optimal adsorption capacities achieved within 120 min. The adsorption performance is attributed to a combination of physical adsorption, due to the microporous structure and large surface area, and chemical adsorption, facilitated by functional groups on the carbon surface. This study demonstrates that *H. verticillata*-derived activated carbon is a viable, cost-effective and environmentally friendly alternative to traditional adsorbents for heavy metal removal from water, with potential applications in sustainable water treatment solutions.

Keywords: Activated carbon, *Hydrilla verticillata*, Heavy metal adsorption, Water pollution, Surface morphology, Adsorption mechanism, Sustainable adsorbent

Introduction

Water pollution remains one of the most pressing environmental challenges of our time, with profound consequences for ecosystems and human health [1]. Heavy metals, including copper (Cu), lead (Pb), iron (Fe) and zinc (Zn), are particularly concerning due to their persistence and toxicity [2]. Unlike organic contaminants, which can degrade over time, heavy metals do not break down and can accumulate in water bodies, sediments and biological organisms. This persistence allows even trace amounts to pose significant risks, especially as these metals biomagnify through the food chain, amplifying their effects at each trophic level [3].

The sources of heavy metal pollution are varied, encompassing both natural processes and anthropogenic activities. Naturally, heavy metals can leach into water

bodies from mineral deposits and volcanic activity [4]. However, human activities have significantly exacerbated the problem. Mining operations, for example, can lead to acid mine drainage, releasing high concentrations of heavy metals into rivers and streams [5]. Similarly, industrial discharges from metal plating, battery manufacturing and electronics industries contribute substantially to heavy metal contamination. Agricultural runoff and improper waste disposal further compound the issue, leading to widespread environmental and health concerns [6].

The presence of heavy metals in water has severe implications for both aquatic ecosystems and human health. In aquatic environments, heavy metals can disrupt reproductive, nervous and immune systems of fish and other organisms, leading to reduced

biodiversity and altered ecosystem dynamics [3]. The accumulation of these metals in aquatic organisms not only affects their health but also poses risks to predators, including birds and mammals, that rely on these organisms for food [7]. This biomagnification process results in higher concentrations of heavy metals at each trophic level, exacerbating the impact on entire ecosystems.

Human health is equally at risk from heavy metal contamination. Consuming water contaminated with metals such as lead can lead to serious health issues, particularly in children, including neurodevelopmental disorders and learning disabilities [8]. In adults, lead exposure is associated with cardiovascular problems and kidney damage [2]. Copper, while essential in trace amounts, can cause gastrointestinal distress and liver damage at higher concentrations [9]. Excessive zinc intake can lead to stomach cramps and interfere with the absorption of other essential minerals [10]. Thus, effective removal of heavy metals from contaminated water is crucial for protecting public health.

Addressing heavy metal contamination requires effective and sustainable solutions. Traditional adsorbents, such as activated carbon derived from coal [11], peat [12] and wood [13], have been widely used due to their high surface area and adsorption capacity. These materials have demonstrated significant effectiveness in removing metals like lead and copper. However, their high cost and environmental impact drive the search for more sustainable alternatives. Recent research has focused on utilizing agricultural and industrial by-products as low-cost adsorbents such as rice husks, sawdust and coconut shells have shown promise, achieving comparable or superior performance to conventional activated carbon [14,15].

Despite advancements with these alternative adsorbents, there are still notable gaps in the research, particularly regarding specific plant-based materials [16]. One such material is *H. verticillata*, an invasive aquatic plant [17]. While plant-derived activated carbons have shown potential, research on *H. verticillata* remains limited. Investigating this plant's potential for producing activated carbon and understanding its adsorption mechanisms could provide valuable insights and address the need for more sustainable water treatment solutions.

The primary aim of this research is to evaluate the adsorption capabilities of activated carbon derived from *H. verticillata* for removing heavy metals such as copper, lead, iron and zinc from aqueous solutions. This study seeks to assess the effectiveness of this plant-based activated carbon in capturing and immobilizing heavy metal ions, thus reducing their concentration in contaminated water. By exploring the adsorption performance of *H. verticillata*-derived activated carbon, we aim to establish its potential as a cost-effective and environmentally friendly alternative to traditional adsorbents.

Understanding the adsorption mechanism is crucial for optimizing the use of *H. verticillata*-derived activated carbon in practical applications. The adsorption process involves complex interactions between the adsorbent's surface and the heavy metal ions, influenced by factors such as surface area, pore structure and functional groups. Elucidating these mechanisms will enhance our ability to improve the performance and selectivity of the adsorbent. Furthermore, determining the effect of varying adsorption times is essential for practical implementation, as adsorption efficiency can vary with time. By examining how adsorption capacity changes over intervals of 15, 30, 45, 60, 90 and 120 min, this study aims to identify optimal contact times for maximum heavy metal removal, balancing efficiency with operational considerations.

The significance of this research extends beyond academic interest, addressing urgent environmental and public health concerns. Effective removal of heavy metals is critical for safeguarding ecosystems and human health. *H. verticillata*, as an invasive species, offers an environmentally beneficial use when converted into activated carbon, transforming a problematic plant into a valuable resource for pollution mitigation. By advancing our understanding of its adsorption capabilities and mechanisms, this research contributes to the development of sustainable water treatment solutions, supporting the global effort to ensure clean and safe water for all.

Materials and method

H. verticillata-derived activated carbon preparation

H. verticillata plants were washed, sun-dried and carbonized at 300 °C for 1 h. To ensure complete drying, the samples were monitored for moisture content using a moisture analyzer until no further weight loss was observed. The resulting char was ground and sieved through a 200 mesh sieve. The powder underwent chemical activation by soaking in 1 M HCl at a 1:10 (w/v) ratio for 4 h, followed by treatment with 1 M NaOH and washing with distilled water until neutral pH was achieved. It was then dried at 105 °C for 3 h. Hydrothermal treatment was performed at 180 °C for 12 h, after which the product was filtered and dried again at 105 °C for 4 h to produce activated carbon.

Characterization

The surface morphology of the *H. verticillata*-derived activated carbon was examined using Scanning Electron Microscopy (SEM) JEOL 6510LV. Raman spectroscopy was conducted using a Fourier Transform Infrared (FTIR) Spectrometer, specifically the Agilent Cary 670, operating within the spectral range of 9,000 - 375 cm⁻¹. To confirm the amorphous nature of the activated carbon structure, X-ray Diffraction (XRD) analysis was performed using a Bruker D8 Advance diffractometer. The specific surface area, pore diameter and total pore volume of the activated carbon were determined using a surface area analyzer (SAA), the Quantachrome Novatouch LX4.

Adsorption test

Heavy metal solutions (Cu, Pb, Fe and Zn) were prepared using distilled water and pro-analysis grade reagents from Merck. The preparation process for these solutions is detailed in the supplementary data to ensure reproducibility and to address any queries about their similarity to solutions from public water systems. The adsorption tests were carried out by adding 0.5 g of *H. verticillata*-derived activated carbon powder to 100 mL of each heavy metal solution. The mixtures were placed on a rotary shaker set to 300 rpm. Adsorption experiments were conducted at varying contact times: 15, 30, 45, 60, 90 and 120 min. At each time interval, samples were withdrawn to analyze the remaining concentration of heavy metals in the solution and

determine the adsorption efficiency of the activated carbon. After each experimental time interval, the adsorbent was separated from the metal solution using a centrifuge set to 4,000 rpm for 10 min, resulting in an adsorbent precipitate. The concentration of heavy metals in the solution was then measured using Atomic Absorption Spectroscopy (AAS) with an Innotech IFX-310320 spectrometer. The adsorption capacity (q), expressed in mg/g and the percentage of adsorption (q_a) were calculated using Eqs. (1) and (2) [18]. In these equations, C_0 represents the initial concentration of metal ions in the solution (mg/L), V is the volume of the solution (L), C_1 is the concentration of metal ions at equilibrium (mg/L), and W is the mass of the adsorbent (g).

$$q = \frac{(C_0 - C_1)}{W} \times V \quad (1)$$

$$q_a = \left[\frac{(C_0 - C_1)}{C_0} \right] \times 100 \quad (2)$$

Results and discussion

Surface morphology

Figure 1(A) illustrates the SEM image of the activated carbon before hydrothermal treatment. The surface morphology is characterized by a rough and undulating structure, indicating a highly irregular surface. This irregularity likely enhances adsorption processes by increasing the available surface area. The structure shows partial adhesion and overlapping of carbon particles, suggesting aggregation. The disordered grain structure further contributes to the complex surface topology, which is associated with enhanced adsorption capacities due to the increased availability of active sites.

Figure 1(B) presents the EDX spectrum of the pre-hydrothermal sample, revealing a carbon content of 88.73 % by mass. This high carbon content suggests the predominance of carbon, which is essential for adsorption. The minimal presence of other elements indicates low impurity levels, advantageous for maintaining high adsorption efficiency. **Figure 1(C)** shows the SEM image of the activated carbon after hydrothermal treatment. The surface morphology exhibits significant changes, appearing relatively smoother with a more uniform texture [19]. This suggests that the hydrothermal process has modified the

surface structure, potentially enhancing adsorption capabilities by uniformly exposing more active sites. The particle diameters are smaller and more consistent, reflecting reduced size heterogeneity. Additionally, the grain orientation is more organized, with a mesh-like structure that facilitates better interaction with heavy metal ions due to increased regularity and accessibility of adsorption sites.

Figure 1(D) presents the EDX spectrum of the post-hydrothermal sample, indicating a carbon content of 94.92 % by mass. This slight increase in carbon content suggests further purification of the carbon structure, potentially removing impurities and enhancing the overall quality of the activated carbon.

The higher carbon content implies a greater presence of active carbon sites available for heavy metal ion adsorption. The observed smoother and more structured surface morphology, along with the increased carbon content, indicates that the hydrothermal treatment has significantly improved the physical properties of the *H. verticillata*-derived activated carbon. The smoother surface may reduce resistance to mass transfer, allowing heavy metal ions to access the adsorption sites more readily. The smaller and more uniform particle sizes could enhance the packing density of the adsorbent, increasing the overall surface area available for adsorption.

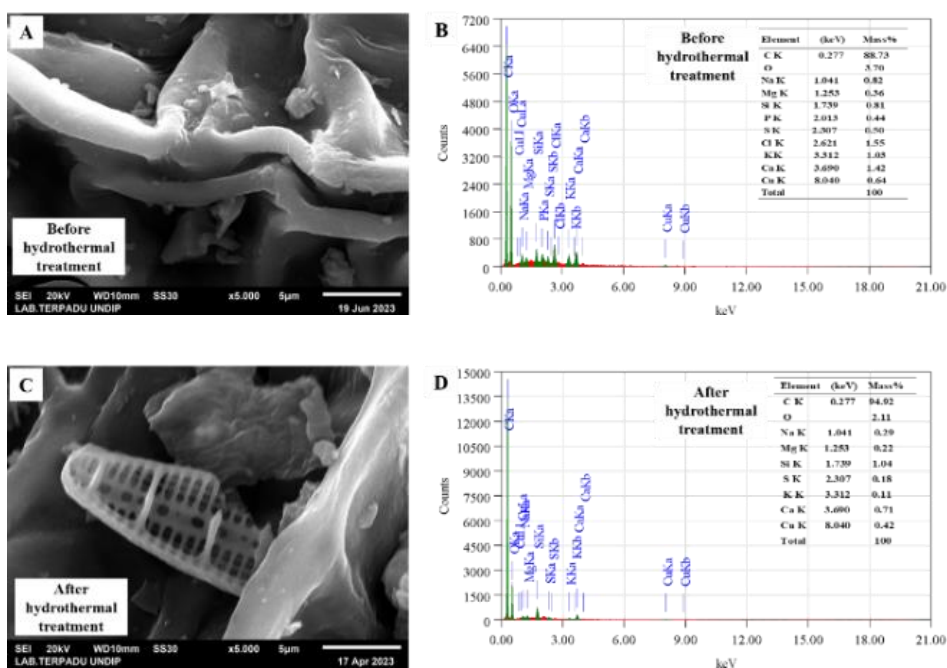


Figure 1 SEM image at a magnification of 5,000 times, and EDX spectrum of *H. verticillata*-derived activated carbon before (A), (B) and after hydrothermal treatment (C), (D).

XRD analysis

The XRD analysis of the hydrothermally treated *H. verticillata*-derived activated carbon reveals key insights into its crystallographic structure. Figure 2 show XRD diffraction pattern of hydrothermally treated *H. verticillata*-derived activated carbon. The diffraction pattern shows a prominent broad peak at 2θ values between 20.96 and 24.06° , which corresponds to the (002) plane of graphite, indicating a disordered or amorphous graphite structure. This broad peak is characteristic of activated carbon and suggests a high

degree of disorder and lack of long-range order in the carbon matrix, which is beneficial for adsorption applications as it implies a greater number of active sites for heavy metal adsorption. In addition to the broad peak, there is a smaller peak observed at $2\theta = 43.79^\circ$, indicative of a minor crystalline region within the otherwise amorphous structure. This small crystalline area suggests that there are some regions within the carbon matrix that have retained a more ordered structure, although these are not predominant.

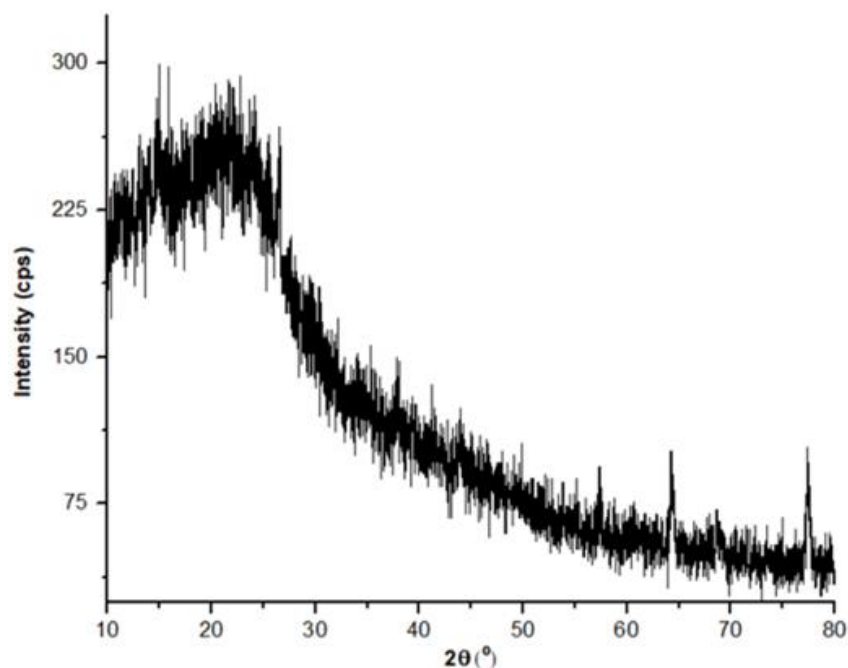


Figure 2 XRD diffraction pattern of hydrothermally treated *H. verticillata*-derived activated carbon.

The presence of additional peaks at 2θ values of 57.38, 64.30 and 77.28 ° indicates the presence of crystalline phases, which are likely due to impurities or contaminants introduced during the activated carbon manufacturing process. The peak at $2\theta = 57.38$ ° is typically associated with materials that possess a crystalline phase, while the peaks at 64.30 and 77.28 ° may indicate the presence of other compounds or elements, possibly introduced by the equipment used during synthesis or analysis.

The overall XRD pattern, with its dominant broad peak and lack of sharp peaks, confirms that the hydrothermally treated *H. verticillata*-derived activated carbon predominantly exhibits an amorphous structure. This amorphous nature is advantageous for adsorption applications as it enhances the availability of active sites and increases the material's capacity to adsorb heavy metal ions [20]. The disordered structure provides more

surface area and pore volume, facilitating the interaction and capture of contaminants from aqueous solutions. This structural characteristic underscores the potential of hydrothermally treated *H. verticillata*-derived activated carbon as an effective and efficient adsorbent for environmental remediation.

FTIR analysis

Figure 3 displays the FTIR spectrum of the activated carbon before hydrothermal treatment, showing several characteristic absorption bands. Before hydrothermal treatment, the FTIR spectrum shows several characteristic absorption bands. The peaks in the region of 1,154.16 - 1,058.32 cm^{-1} correspond to C-O stretching vibrations, further confirming the presence of carbonyl groups. Additionally, the peak at 595.39 cm^{-1} indicates the presence of O-H bending in alcohol groups.

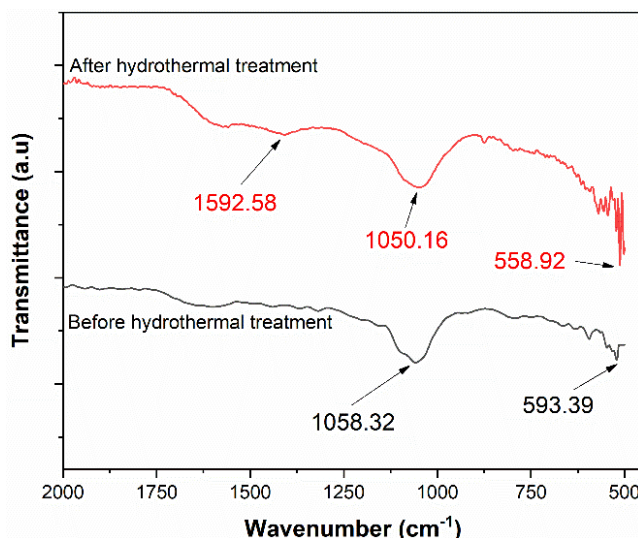


Figure 3 FTIR spectra of *H. verticillata*-derived activated carbon samples before and after hydrothermal treatment.

After hydrothermal treatment, the FTIR spectrum shows noticeable shifts and the appearance of new absorption bands, indicating changes in the surface chemistry due to the carbonization and chemical activation processes. A significant change is the appearance of a peak at $1,592.58\text{ cm}^{-1}$, attributed to the C=O stretching vibration in carbonyl groups, such as ketones, aldehydes and carboxylic acids. This indicates the formation of new oxygen-containing functional groups, which are crucial for the adsorption process by providing sites for chemical interaction with heavy metal ions. The C-O stretching vibration band shifts slightly to $1,150.08 - 1,050.16\text{ cm}^{-1}$. These shifts reflect changes in the chemical environment of these functional groups, likely enhancing the adsorbent's capacity to interact with heavy metal ions (ref). The peak at 558.92 cm^{-1} indicates the continued presence of O-H bending in alcohol groups. This suggests that while the surface chemistry undergoes significant changes, some functional groups remain stable.

The retention and appearance of new functional groups after hydrothermal treatment suggest that the activated carbon retains and enhances its essential chemical characteristics, potentially improving its adsorption properties. The presence of carbonyl and aromatic groups is crucial for the adsorption process, as they can form coordination bonds with heavy metal ions, facilitating their removal from aqueous solutions (ref). The increased carbon content and structural changes indicated by the FTIR spectra align with the XRD and EDX findings, reinforcing the potential of

hydrothermally treated *H. verticillata*-derived activated carbon as an effective adsorbent for heavy metals.

Pore characteristic

The nitrogen adsorption-desorption isotherm of *H. verticillata*-derived activated carbon, as depicted in **Figure 4(A)**, alongside the BJH curve in **Figure 4(B)**, provides crucial insights into its pore characteristics. The Brunauer-Emmett-Teller (BET) analysis indicates a surface area of $72.802\text{ m}^2/\text{g}$. The total pore volume of this activated carbon is $0.1011\text{ cm}^3/\text{g}$, with a pore diameter of 0.2776 nm , classifying it as microporous since microporous materials have pore diameters less than 2 nm . Comparatively, *H. verticillata*-derived activated carbon demonstrates superior pore characteristics over other biomass-derived activated carbons. For instance, bamboo-derived activated carbon, carbonized using a microwave process, has a pore volume of $0.049\text{ cm}^3/\text{g}$ and a pore size of 2.91 nm , classifying it as mesoporous. Similarly, lemon-derived activated carbon has a pore volume of $0.649\text{ cm}^3/\text{g}$ and a pore diameter of 0.12 nm . The specific surface area of bamboo-derived activated carbon was $240.09\text{ m}^2/\text{g}$.

Despite the lower surface area of *H. verticillata*-derived activated carbon ($72.802\text{ m}^2/\text{g}$) compared to bamboo-derived activated carbon, the microporous nature of *H. verticillata*-derived activated carbon makes it highly effective for adsorbing small molecules, including heavy metal ions. Microporous activated carbons are highly valued for their large surface area and selectivity in adsorbing small molecules, which makes

them particularly effective for heavy metal adsorption applications. A high surface area is crucial for an effective adsorbent, as it provides more active sites for

the adsorption of heavy metal ions from aqueous solutions.

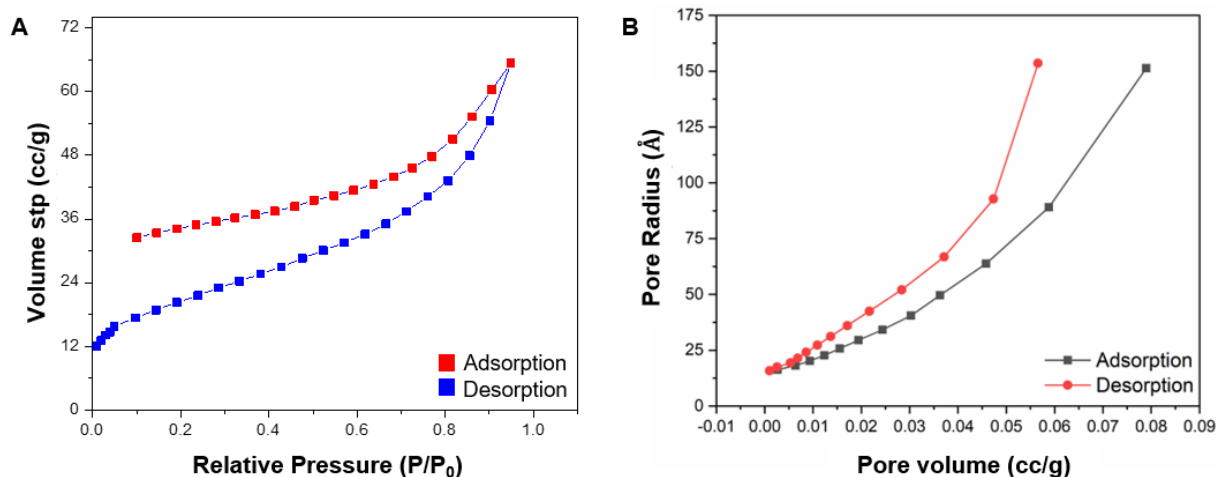


Figure 4 Nitrogen adsorption-desorption isotherm of *H. verticillata*-derived activated carbon.

The BJH adsorption curve indicates the pore volume distribution within the sample. The pore volume increases with pore radius, reaching a maximum of $0.079 \text{ cm}^3/\text{g}$ at a radius of 151.3893 \AA . The desorption curve, on the other hand, shows the reduction in pore volume as the pores empty. Both curves demonstrate that the *H. verticillata*-derived activated carbon has a well-developed microporous structure, essential for effective adsorption [21]. Despite the surface area in this study being lower than that of some other activated carbons, such as bamboo-derived activated carbon ($240.09 \text{ m}^2/\text{g}$), the pore size and volume are optimized for heavy metal adsorption. The smaller pores and higher proportion of micropores in *H. verticillata*-derived activated carbon allow for a high density of active sites, making it a potent adsorbent for heavy metal ions. This balance of surface area, pore volume and pore size distribution ensures effective adsorption performance, making *H. verticillata*-derived activated carbon a viable and sustainable alternative for water treatment applications [17].

Adsorption performance

The adsorption performance of *H. verticillata*-derived activated carbon was evaluated by examining its ability to remove 4 heavy metals (Cu, Fe, Pb and Zn) from aqueous solutions over different contact times. **Figure 5(A)** illustrates the relationship between contact

time and the percentage of heavy metals absorbed. The adsorption lines did not start at 0.0 because there is an initial adsorption that occurs almost instantaneously when the activated carbon is added to the solution. This rapid initial uptake is typical and indicates the high reactivity of the surface sites. For instance, the removal efficiency for copper (Cu) starts at 44.17 % at 15 min and reaches 56.14 % at 120 min. Similarly, lead (Pb) shows the highest removal efficiency among the 4 metals, starting at 89.42 % and increasing to 94.61 % over the same period. This trend indicates that longer contact times allow more metal ions to be captured by the active sites of the activated carbon, enhancing overall adsorption efficiency.

The observed trend in the removal efficiencies of $\text{Pb} > \text{Fe} > \text{Cu} > \text{Zn}$ can be attributed to several factors, including the affinity of the activated carbon for different metal ions and the specific properties of each metal ion. Lead (Pb) demonstrates the highest removal efficiency due to its larger ionic radius and higher electronegativity, which likely increases its interaction with the active sites on the activated carbon. Furthermore, the strong affinity between lead ions and the functional groups present on the carbon surface enhances its adsorption.

Iron (Fe) follows lead in removal efficiency. The presence of Fe in multiple oxidation states can facilitate various adsorption mechanisms, including ion exchange

and surface complexation, which contributes to its relatively high adsorption capacity. Copper (Cu) has a moderate removal efficiency compared to lead and iron. The interaction of copper ions with the active sites on the activated carbon is strong but less pronounced than that of lead and iron [22], which could be due to the smaller ionic radius and lower electronegativity of

copper ions. Zinc (Zn) exhibits the lowest removal efficiency among the 4 metals. This can be attributed to its smaller ionic radius and lower affinity for the active sites on the activated carbon. Additionally, the competition between zinc ions and other metal ions for adsorption sites may further reduce its removal efficiency.

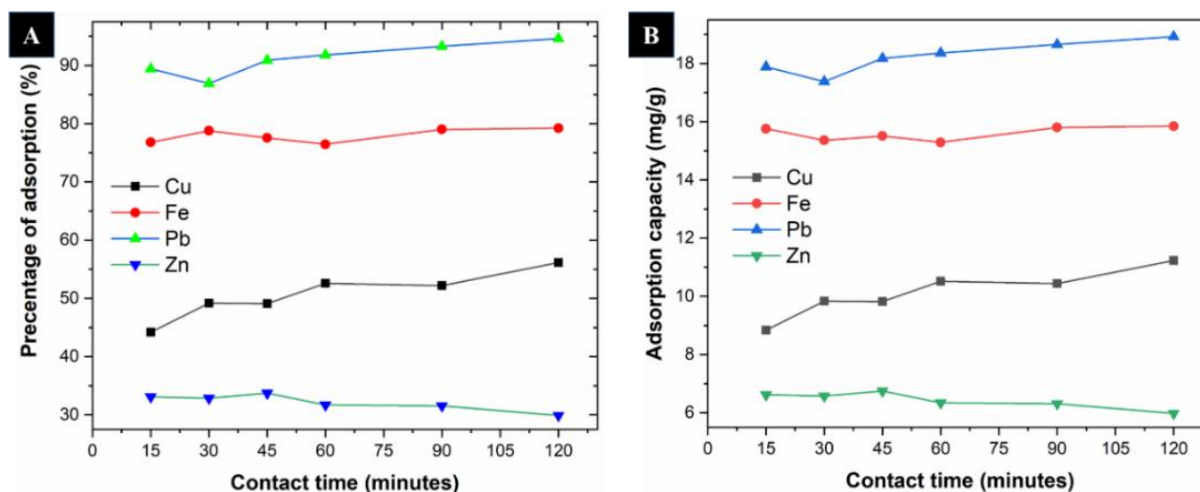


Figure 5 The percentage of adsorption (A), and adsorption capacity (B) of *H. verticillata*-derived activated carbon.

Figure 5(B) depicts the adsorption capacity of the activated carbon for the same heavy metals over time. The adsorption capacity for copper increased from 8.8344 mg/g at 15 min to 11.2276 mg/g at 120 min. Lead showed superior adsorption, rising from 17.884 to 18.9218 mg/g, due to the micro-sized pores and high surface area of the activated carbon. Zinc, however, exhibited a decrease in adsorption percentage from 33.08 to 29.90 % and capacity from 6.6162 to 5.97998 mg/g over the same period. This indicates a preferential adsorption tendency of the *H. verticillata* activated carbon towards certain heavy metals, aligning with the properties of biomass-derived activated carbons where surface chemistry and pore structure are crucial [23].

The high carbon content on the surface of *H. verticillata* activated carbon, as confirmed by EDX analysis, facilitate strong interactions with metal ions, leading to higher adsorption efficiencies and capacities. The time was limited to a maximum of 120 min as preliminary tests indicated that significant adsorption occurred within this time frame. While the adsorption of Pb and Cu was still increasing at 120 min, the focus was on establishing a baseline performance within a practical timeframe for comparative studies. Extending

the contact time beyond 120 min could be explored in future research to fully understand the equilibrium state.

The performance of commercial activated carbons (CAC) typically exhibits adsorption capacities of 15.0 mg/g for Pb and 14.0 mg/g for Cu [24]. Competitive adsorption results demonstrated that the adsorption ability of sorbents is restricted by the presence of other ions, leading to decreased performance compared to single-ion sorption scenarios. The adsorption capacities observed in this study, especially for lead and copper, are within this range, demonstrating that *H. verticillata* activated carbon is a viable alternative [18].

Adsorption mechanism

The adsorption mechanism of heavy metals onto *H. verticillata*-derived activated carbon can be understood through a detailed examination of the physical and chemical interactions between the adsorbent and the adsorbates. Physical adsorption, or physisorption, involves the adherence of heavy metal ions onto the surface of the activated carbon primarily through van der Waals forces [25]. These are weak, non-specific interactions that occur due to the induced dipole moments between the adsorbent and the adsorbate. The

large surface area and porous structure of activated carbon, as determined through BET analysis, provide ample sites for physical adsorption. The microporous nature of the *H. verticillata*-derived activated carbon, with its high surface area, suggests a significant potential for physisorption [26]. The small pore diameters allow for the capture of metal ions through size-exclusion effects, enhancing the overall adsorption capacity [27].

Chemical adsorption or chemisorption involves the formation of stronger, more specific interactions between the adsorbent and the adsorbate, such as covalent or ionic bonds [28]. The FTIR analysis indicates the presence of various functional groups on the surface of the activated carbon, including hydroxyl (OH), carbonyl (C=O) and aromatic (C=C) groups, that can interact with heavy metal ions through mechanisms such as ion exchange, complexation and coordination bonding [29]. For instance, the hydroxyl groups can donate electrons to form coordination bonds with metal cations, while carbonyl groups can participate in complexation reactions, effectively immobilizing the metal ions on the carbon surface [30].

The adsorption process observed in *H. verticillata*-derived activated carbon is likely a combination of both physical and chemical adsorption. Initially, metal ions may be attracted to the surface through van der Waals forces, which are characteristic of physisorption [31]. Once in close proximity to the surface, the metal ions can form stronger interactions with the functional groups present on the activated carbon, characteristic of chemisorption. This dual mechanism enhances the overall adsorption capacity and efficiency [32]. Heavy metal ions in the aqueous solution initially diffuse towards the surface of the activated carbon [33]. The high surface area and microporous structure of the activated carbon facilitate this initial contact through physical adsorption, where the metal ions are attracted to the surface of the carbon [34].

Upon contact, the metal ions interact with the functional groups present on the activated carbon surface. Hydroxyl, carbonyl and aromatic groups play a significant role in binding the metal ions. These interactions are primarily through chemical adsorption mechanisms, where chemical bonds are formed between the metal ions and the functional groups on the carbon surface. Functional groups such as OH and C=O form

complexes and coordination bonds with the metal ions, leading to their immobilization on the carbon surface. This complexation process is enhanced by the carbon's amorphous structure, which provides a greater number of active sites for adsorption, thereby increasing the efficiency of the adsorbent. Once the metal ions are adsorbed, they are stabilized on the carbon surface, reducing their mobility and preventing desorption under normal conditions. This stabilization is crucial for ensuring the long-term effectiveness of the adsorbent in water treatment applications, as it ensures that the heavy metals remain bound to the activated carbon and do not re-enter the aqueous solution.

Conclusions

The study evaluated the efficacy of activated carbon derived from *H. verticillata* for adsorbing heavy metals (Cu, Pb, Fe and Zn). Hydrothermal treatment significantly improved the carbon's surface area (72.802 m²/g) and microporous structure (pore diameter of 0.2776 nm), enhancing its adsorption properties. The carbon content was 88.73 % by mass. Adsorption capacities were 11.2276 mg/g for Cu and 18.9218 mg/g for Pb, with removal efficiencies of 56.14 and 94.61 %, respectively. These results show that *H. verticillata*-derived activated carbon is a sustainable and effective alternative for heavy metal removal, performing competitively with commercial activated carbons, which have capacities of 15.0 mg/g for Pb and 14.0 mg/g for Cu.

References

- [1] H Xu, Y Jia, Z Sun, J Su, QS Liu, Q Zhou and G Jiang. Environmental pollution, a hidden culprit for health issues. *Eco-Environment & Health* 2022; **1(1)**, 31-45.
- [2] A Alengebawy, ST Abdelkhalek, SR Qureshi and MQ Wang. Heavy metals and pesticides toxicity in agricultural soil and plants: Ecological risks and human health implications. *Toxics* 2021; **9(3)**, 42.
- [3] MM Uddin, MCM Zakeel, JS Zavahir, FMMT Marikar and I Jahan. Heavy metal accumulation in rice and aquatic plants used as human food: A general review. *Toxics* 2021; **9(12)**, 360.
- [4] Z Wang, P Luo, X Zha, C Xu, S Kang, M Zhou, D Nover and Y Wang. Overview assessment of risk evaluation and treatment technologies for heavy

- metal pollution of water and soil. *Journal of Cleaner Production* 2022; **379(2)**, 134043.
- [5] N Akhtar, MI Syakir Ishak, SA Bhawani and K Umar. Various natural and anthropogenic factors responsible for water quality degradation: A review. *Water* 2021; **13(19)**, 2660.
- [6] J Shi, W Huang, H Han and C Xu. Pollution control of wastewater from the coal chemical industry in China: Environmental management policy and technical standards. *Renewable and Sustainable Energy Reviews* 2021; **143**, 110883.
- [7] DA Ayejoto and JC Egbueri. Human health risk assessment of nitrate and heavy metals in urban groundwater in Southeast Nigeria. *Ecological Frontiers* 2024; **44(1)**, 60-72.
- [8] S Madhav, A Ahamad, AK Singh, J Kushawaha, JS Chauhan, S Sharma and P Singh. *Water pollutants: Sources and impact on the environment and human health*. In: D Pooja, P Kumar, P Singh and S Patil (Eds.). Sensors in water pollutants monitoring: Role of material. Springer, Singapore, 2020, p. 43-62.
- [9] A Taylor, JS Tsuji, MR Garry, ME McArdle, WL Goodfellow, WJ Adams and CA Menzie. Critical review of exposure and effects: Implications for setting regulatory health criteria for ingested copper. *Environmental Management* 2020; **65(1)**, 131-159.
- [10] H Schoofs, J Schmit and L Rink. Zinc toxicity: Understanding the limits. *Molecules* 2024; **29(13)**, 3130.
- [11] C Zhao, L Ge, L Mai, X Li, S Chen, Q Li, S Li, L Yao, Y Wang and C Xu. Review on coal-based activated carbon: Preparation, modification, application, regeneration, and perspectives. *Energy & Fuels* 2023; **37(16)**, 11622-11642.
- [12] M Wiśniewska and P Nowicki. Peat-based activated carbons as adsorbents for simultaneous separation of organic molecules from mixed solution of poly (acrylic acid) polymer and sodium dodecyl sulfate surfactant. *Colloids and Surfaces A: Physicochemical and Engineering Aspects* 2020; **585**, 124179.
- [13] H Jiao, X Guo, F Shu, Q Zhang, W Wu, Y Jin and B Jiang. Structure-property-function relationships of wood-based activated carbon in energy and environment materials. *Separation and Purification Technology* 2024; **353**, 128607.
- [14] N Hossain, MA Bhuiyan, BK Pramanik, S Nizamuddin and G Griffin. Waste materials for wastewater treatment and waste adsorbents for biofuel and cement supplement applications: A critical review. *Journal of Cleaner Production* 2020; **255**, 120261.
- [15] G Ramalingam, AK Priya, L Gnanasekaran, S Rajendran and TKA Hoang. Biomass and waste derived silica, activated carbon and ammonia-based materials for energy-related applications - a review. *Fuel* 2024; **355**, 129490.
- [16] MA Tony. Low-cost adsorbents for environmental pollution control: A concise systematic review from the prospective of principles, mechanism and their applications. *Journal of Dispersion Science and Technology* 2022; **43(11)**, 1612-1633.
- [17] N Kumar. *Hydroponics and environmental bioremediation: Wastewater treatment*. Springer Nature, Cham, Switzerland, 2024.
- [18] A Kali, A Amar, I Loulidi, M Jabri, C Hadey, H Lgaz, AA Alrashdi and F Boukhlifi. Characterization and adsorption capacity of four low-cost adsorbents based on coconut, almond, walnut, and peanut shells for copper removal. *Biomass Conversion and Biorefinery* 2024; **14(3)**, 3655-3666.
- [19] E Sembiring, D Bonardo, K Sembiring and Z Sitorus. Analyze the strength of ceramics made from clay, Sinabung volcanic ash and sea water in the term of the structure. *Journal of Physics: Conference Series* 2021; **2019**, 012066.
- [20] NA Awang, WNW Salleh, F Aziz, N Yusof and AF Ismail. A review on preparation, surface enhancement and adsorption mechanism of biochar-supported nano zero-valent iron adsorbent for hazardous heavy metals. *Journal of Chemical Technology & Biotechnology* 2023; **98(1)**, 22-44.
- [21] B Wang, J Lan, C Bo, B Gong and J Ou. Adsorption of heavy metal onto biomass-derived activated carbon. *RSC Advances* 2023; **13(7)**, 4275-4302.
- [22] D Bonardo, N Darsono, S Humaidi, A Imaduddin and NS Silalahi. Effect of calcination frequency on the thermoelectric properties of Ti doped CuCrO₂ by solid state method. *Journal of Metals, Materials and Minerals* 2023; **33(4)**, 1785.

- [23] F Zhi, W Zhou, J Chen, Y Meng, X Hou, J Qu, Y Zhao and Q Hu. Adsorption properties of active biochar: Overlooked role of the structure of biomass. *Bioresource Technology* 2023; **387**, 129695.
- [24] R Shahrokhi-Shahraki, C Benally, MG El-Din and J Park. High efficiency removal of heavy metals using tire-derived activated carbon vs commercial activated carbon: Insights into the adsorption mechanisms. *Chemosphere* 2021; **264**, 128455.
- [25] Z Raji, A Karim, A Karam and S Khalloufi. Adsorption of heavy metals: Mechanisms, kinetics, and applications of various adsorbents in wastewater remediation - a review. *Waste* 2023; **1(3)**, 775-805.
- [26] NS Razali, AS Abdulhameed, AH Jawad, ZA ALOthman, TA Yousef, OK Al-Duaij and NS Alsaiani. High-surface-area-activated carbon derived from mango peels and seeds wastes via microwave-induced $ZnCl_2$ activation for adsorption of methylene blue dye molecules: Statistical optimization and mechanism. *Molecules* 2022; **27(20)**, 6947.
- [27] RA Ningrum, S Humaidi, S Sihotang, D Bonardo and Estananto. Synthesis and material characterization of calcium carbonate ($CaCO_3$) from the waste of chicken eggshells. *Journal of Physics: Conference Series* 2022; **2193(1)**, 012009.
- [28] EG Söğüt and M Gülcan. *Adsorption: Basics, properties, and classification*. In: C Verma, J Aslam and ME Khan (Eds.). Adsorption through advanced nanoscale materials. Elsevier, Amsterdam, Netherlands, 2023, p. 3-21.
- [29] M Raninga, A Mudgal, VK Patel, J Patel and MK Sinha. Modification of activated carbon-based adsorbent for removal of industrial dyes and heavy metals: A review. *Materials Today: Proceedings* 2023; **77**, 286-294.
- [30] Y Fei and YH Hu. Design, synthesis, and performance of adsorbents for heavy metal removal from wastewater: A review. *Journal of Materials Chemistry A* 2022; **10(3)**, 1047-1085.
- [31] ED Ligneris, LF Dumée and L Kong. Nanofibers for heavy metal ion adsorption: Correlating surface properties to adsorption performance, and strategies for ion selectivity and recovery. *Environmental Nanotechnology, Monitoring & Management* 2020; **13**, 100297.
- [32] Z Zhang, T Wang, H Zhang, Y Liu and B Xing. Adsorption of Pb (II) and Cd (II) by magnetic activated carbon and its mechanism. *Science of the Total Environment* 2021; **757**, 143910.
- [33] X Liu, X Xu, X Dong and J Park. Competitive adsorption of heavy metal ions from aqueous solutions onto activated carbon and agricultural waste materials. *Polish Journal of Environmental Studies* 2020; **29(1)**, 749-761.
- [34] M Sultana, MH Rownok, M Sabrin, MH Rahaman and SMN Alam. A review on experimental chemically modified activated carbon to enhance dye and heavy metals adsorption. *Cleaner Engineering and Technology* 2022; **6**, 100382.